Matter

CellPress

Article

Versatile and efficient photopolymerization approach to zinc oxide-composed dual functional membranes for sustainable water treatment

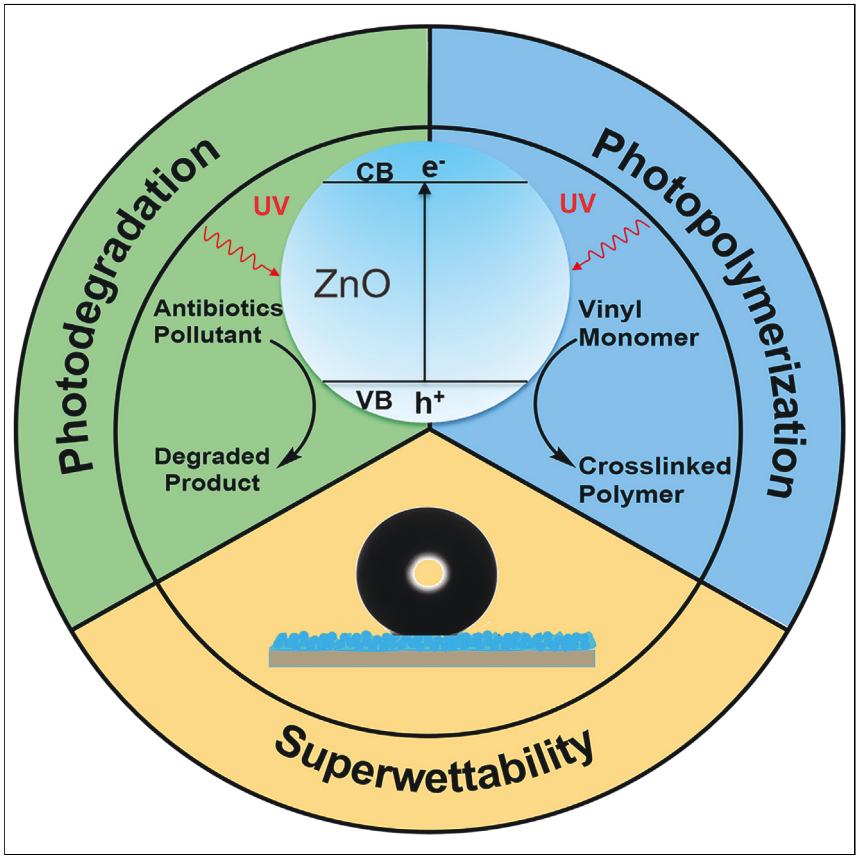

We developed a zinc oxide (ZnO)–initiated photopolymerization strategy to fabricate superhydrophilic composite hydrogel coatings or membranes for water-cleaning applications. The integrated advantages of the photocatalytic properties and the nanoscale morphology of ZnO nanoparticles render this method cost-effective, sustainable, versatile, and scalable. Three types of ZnO/hydrogel composite membranes are fabricated via this strategy for the separation of stratified oil/water mixtures, removal of nanoscale oil emulsions from water, and one-step removal of emulsions and dissolved pollutants, respectively.

4 **Demonstrate**
Proof-of-concept of performance with intended application/response

Chenxuan Li, Boliang Jiangli, Brian Lee, ..., Mohammad Al-Hashimi, Sarbajit Banerjee, Lei Fang

fang@chem.tamu.edu

Highlights

Multiple functions of ZnO nanoparticles for membrane water treatment

Spatially controlled, scalable, cost-effective, versatile photopolymerization

Membrane featuring superhydrophilicity and photocatalytic activity

Simultaneous removal of oils and dissolved organic pollutants from water

Li et al., Matter 7, 1146–1160
March 6, 2024
https://doi.org/10.1016/j.matt.2023.12.033

CellPress

Matter

Article

Versatile and efficient photopolymerization approach to zinc oxide-composed dual functional membranes for sustainable water treatment

Chenxuan Li,[1] Boliang Jiangli,[2] Brian Lee,[1] Guanghua Yu,[1] Wan Zhang,[1] Hengxi Chen,[2] Sarah Sanders,[1] Mohammad Al-Hashimi,[3] Sarbajit Banerjee,[1,2] and Lei Fang[1,2,4,*]

SUMMARY

Water contaminated with organic pollutants significantly threatens human health and ecosystems. Despite advances in water treatment membranes, challenges persist in their complex fabrication processes and limitations in handling intricate wastewater treatments. Here, we introduce a straightforward, sustainable, scalable, and adaptable strategy for fabricating superwettable membranes using zinc oxide (ZnO)-initiated photopolymerization. ZnO nanoparticles used in this approach provide spatial control for polymerization, enhance surface roughness to induce superhydrophilicity for oil removal, and catalyze photodegradation of dissolved organic contaminants. Versatility of this approach allows the fabrication of three distinct types of membranes, showcasing exceptional performance in diverse water treatment scenarios. Stratified and emulsified oil/water mixtures can be separated efficiently (>99.0%), with fluxes up to 19,700 L $m^{-2}h^{-1}$. In addition, over 90% of soluble organic pollutants can be photodegraded within two filtration cycles, concurrently with oil removal. This membrane-fabricating strategy paves the way for the scalable production of superwettable and photocatalytic membranes for sustainable water treatment applications.

INTRODUCTION

The massive expansion of the intertwined chemical and energy industries encompassing hydrocarbon fuels, chemical precursors, and pharmaceuticals poses risks to human health and vulnerable ecosystems as a result of water contamination by organic pollutants such as dispersed oils and soluble organic compounds including dyes, surfactants, and antibiotics.[1–3] Traditionally, these organic pollutants in water are removed by physical methods such as adsorption,[4] distillation,[5] and electrocoagulation,[6] and chemical methods such as chemical oxidation[7] and flocculation.[8] Compared to these conventional methods, membrane separation offers sustainable advantages such as continuous operation, high efficiency, and low energy input.[9–12] Superwettable membranes possessing opposite affinity to oil and water demonstrate exceptional efficiency in separating immiscible oil/water mixtures.[13–17] Specifically, oil-blocking superhydrophilic and superoleophobic membranes provide several unique advantages for water treatment compared with their water-blocking superhydrophobic and superoleophilic counterparts, including the lower susceptibility to fouling, better suitability for gravity-driven separation, and higher flux owing to the low viscosity of water.[13,15,18] Following the design strategy of imparting surface roughness into high surface energy

PROGRESS AND POTENTIAL

The contamination of freshwater sources with oils, organic solvents, and soluble antibiotics poses significant risks to human health and ecosystems. To address this critical issue, superwettable membranes offer a promising solution for cleaning up water with high separation efficiency and low energy consumption. Nevertheless, the development of simple and scalable methods to fabricate these membranes remains challenging. This paper presents a versatile strategy that uses photopolymerization to create superwettable membranes. The multifunctionality of ZnO nanoparticles lends feasibility, scalability, adaptability, and efficiency to the process. The produced membranes demonstrate remarkable efficiency in various water treatment scenarios. This approach lays the foundation for the fabrication and application of cost-effective membranes for sustainable water purification technologies, especially in developing areas with limited access to water-cleaning facilities.

materials, as elucidated by the Young model[19] and the Cassie-Baxter model,[20,21] a variety of superhydrophilic and underwater superoleophobic membranes have been developed by compositing inorganic nanoparticles such as SiO_2,[22] carbon nanotubes,[23] or graphene oxide,[24] with hydrophilic polymeric materials (e.g., hydrogels).[25–30] These membranes showed excellent performance in removing immiscible oil from water.

To remove dissolved pollutants in water, catalytic degradation processes, particularly semiconductor photodegradation processes, have been developed and applied in water treatment, providing an alternative to traditional adsorption methods. The photodegradation approaches offer the advantage of continuous operation, which is not constrained by the capacity of porous adsorption materials.[31] In this context, incorporating photocatalytic semiconductor nanoparticles (e.g., ZnO,[32,33] TiO_2[34–36]) into membranes allows for the photodegradation of dissolved pollutants under ultraviolet (UV) or sunlight when water passes through the membrane. For example, a ZnO nanorod decorated nanofibrous polyvinylidene fluoride (PVDF) membrane can remove dissolved dyes from water under UV light, and its superhydrophilic nature allows for oil/water separation in an additional step.[32] However, most of these membranes can only work in a conventional batch-type mode with relatively long durations.[33–36] To achieve simultaneous removal of both immiscible oil and dissolved pollutants from water, flow-through catalytic membranes were designed to allow sufficient contact between the membrane and the aqueously dissolved organic pollutant molecules, leading to catalytic photodegradation of these pollutants under continuous operation.[37] Li and coworkers developed a superhydrophilic and underwater superoleophobic membrane by electrochemical deposition of hierarchical TiO_2 nanotubes.[38] The resulting membrane demonstrates efficient flow-through photodegradation of dissolved organic molecules and at the same time can effectively separate layered oil/water mixtures. More recently, there have been developments in the fabrication of membranes that can simultaneously separate oil-in-water emulsions and photocatalytically degrade organic pollutants, such as TiO_2/sulfonated graphene oxide/Ag,[39] hydrogel-PVDF@ZnO/Ag,[40] TiO_2/Co_3O_4/graphene oxide,[41] and Cl/S-g-C_3N_4 membranes.[42] Despite these significant advances, the fabrication of these multifunctional membranes typically requires complex fabrication procedures, limiting the desired large-scale application of these membranes for water treatment. Moreover, such membranes exhibit relatively low efficiency in separating oil/water mixtures solely due to their relatively low flux. Therefore, there is a significant demand for a simple, cost-effective, scalable, and versatile strategy for the general fabrication of superwettable yet photocatalytically active membranes for a broad range of water purification applications. Here, we report a scalable and versatile ZnO-initiated photopolymerization (ZIP) coating strategy to address this challenge. Here, ZnO nanoparticles (ZnONPs) serve multiple functions: as the initiator for photopolymerization during fabrication, as the surface roughening agent for superwettability, and as the photocatalyst for photodegradation of dissolved organic pollutants. The fabrication of various large-area membranes and their applications for specific water treatment scenarios, including stratified oil/water mixtures, surfactant-free or surfactant-stabilized oil-in-water emulsions, and organic pollutant-contaminated water, were demonstrated. The simplicity, cost-effectiveness, low energy input, and versatility of this ZIP approach, together with corresponding high performance in various applications, set this work apart from existing benchmark coating methods, making it an ideal platform technology for the large-scale production of superwettable coatings for wastewater effluent treatment.

[1]Department of Chemistry, Texas A&M University, 3255 TAMU, College Station, TX 77843, USA

[2]Department of Materials Science & Engineering, Texas A&M University, 3003 TAMU, College Station, TX 77843, USA

[3]Department of Chemistry, Texas A&M University at Qatar, P.O. Box 23874, Doha, Qatar

[4]Lead contact

*Correspondence: fang@chem.tamu.edu

https://doi.org/10.1016/j.matt.2023.12.033

RESULTS AND DISCUSSION

Design and fabrication of membranes via the ZIP approach

The central design principle here is based on the dual functions of ZnONPs: their ability to induce a nanoscale, highly rough morphology on the surface for superwettability, and their ability to generate radicals under UV irradiation as a semiconductor. To achieve the desired superhydrophilic and underwater superoleophobic coating suitable for water treatment, we designed composite coatings composed of ZnONPs embedded in photopolymerizable hydrophilic polymer matrices. Polyacrylamide (PAM) was selected as the matrix due to its ease of photopolymerization, intrinsic hydrophilicity, underwater oleophobicity, and environmental friendliness.[25–29] Meanwhile, the presence of ZnONPs (100 or 500 nm average diameter) can lead to a highly rough surface when cast on the substrate. When coated with PAM, the rough surface greatly amplifies the hydrophilicity according to the Wenzel model.[19] If underwater, the rough surface of the ZnONPs/PAM can trap water and lead to small area fraction of the solid-oil interface, resulting in underwater superoleophobicity according to the Cassie-Baxter model.[20,21] ZnONPs also represent a class of excellent non-migratable photoinitiators for polymerizing various vinyl monomers, including acrylamide.[43–46] Here, we use a ZIP approach to synthesize composites of ZnONPs and PAM on various surfaces as coating. During ZIP, selective initiation of photopolymerization on the surface of the ZnONPs ensures excellent spatial control of the formed hydrophilic PAM, which can also serve as the binding matrix of the composite for mechanical robustness .[44] Here, the spatial control of ZIP, limited to the area near the surface of ZnONPs, prevents excessive formation of PAM that could obscure the rough surface features, ensuring that the ZnONPs-induced high surface roughness is maintained for superwettability. Last but not least, the photocatalytic activity of ZnONPs can also be harnessed for the photodegradation of water-dissolved organic contaminants when the aqueous phase is passing through the membrane. Overall, the deployment of these low-cost and multifunctional ZnONPs lead to simple superhydrophilic membrane fabrication processes that are efficient for various monomers, substrates, and applications.

In this study, we showcase three instances of this versatile ZIP technique applied to diverse substrates, resulting in a range of separation membranes suitable for different water treatment applications. Specifically, ZnONPs/hydrogel composites were coated onto a stainless-steel mesh (SSM) with large pore size, coated onto a mixed cellulose ester (MCE) membrane with small pore size, and fabricated as a free-standing membrane.

First, the ZIP coating of SSM by a superhydrophilic/underwater superoleophobic ZnONPs/PAM composite was achieved (Scheme 1A).[26] A 30 × 30 cm SSM with large pore diameter of ~109 μm was used as the substrate to ensure high flux and efficient separation of stratified oil/water mixtures. ZnONPs with an average particle size of ~500 nm were first spray-coated onto the SSM (Figures S1A and S1B) at a coating density of 3.5 mg/cm^2. Subsequently, the entire mesh was immersed in a solution consisting of acrylamide monomer and bis-acrylamide crosslinker, and drawn out from the solution. Due to the high surface area of ZnONPs, the ZnONPs/SSM surface was effectively wetted by the solution, eliminating the need for an adhesive agent or further tuning of the solution viscosity, a common yet tedious procedure in many other coating formulations.[26,47] After simple irradiation of the wet SSM sample under 100 mW/cm^2 UV light at 365 nm for 15 min, the ZIP process involving polymerization of acrylamide took place on the surface of ZnONPs to afford an SSM coated by the composite of ZnONPs and PAM (PAM-ZnO@SSM).

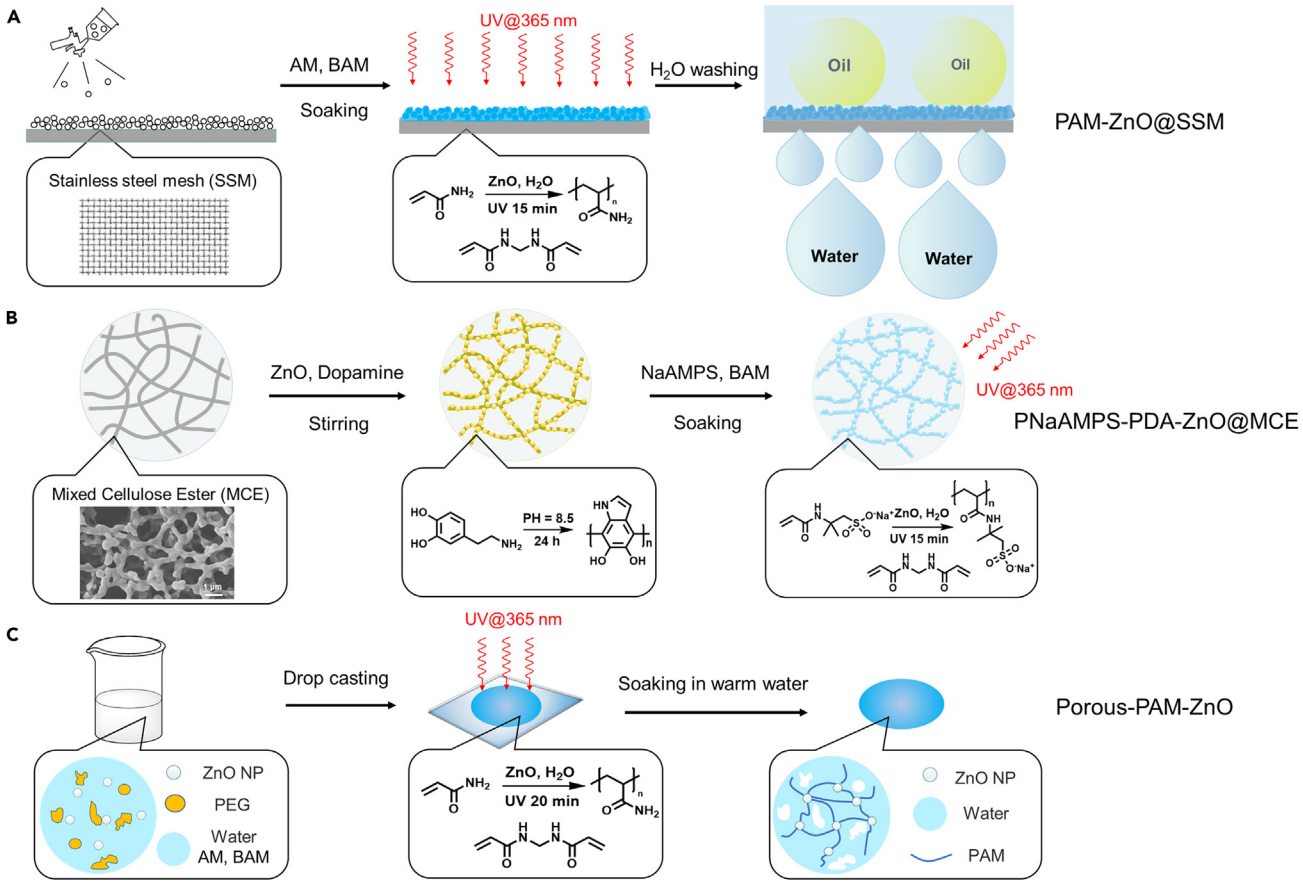

Scheme 1. Fabrication of a variety of superhydrophilic membranes using the ZIP approach

(A) PAM-ZnO@SSM: coating on high flux SSMs.

(B) PNaAMPS-PDA-ZnO@MCE: coating on MCE membranes.

(C) Porous-PAM-ZnO: freestanding porous polyacrylamide-ZnONPs composite membranes.

In a second example, the ZIP method was used to coat a substrate with much smaller pore size, which is good for separating oil-in-water emulsions composed of micrometer/nanometer-scale oil droplets (Scheme 1B). An MCE membrane with interconnected pore structures possessing an average pore size of ~0.45 μm was selected as the substrate. MCE is a widely used hydrophilic membrane for environmental and microbiological filtration due to its low cost, high chemical resistance, and tunable range of pore dimensions.[47–49] ZnONPs with a particle size of ~100 nm (Figures S1C and S1D) were immobilized onto the skeleton of the MCE membrane using polydopamine (PDA), which represents a strong natural adhesive formed through the oxidative polymerization of dopamine under basic conditions in air. Subsequently, the membrane was immersed in a solution of hydrophilic sodium 2-acrylamido-2-methylpropanesulfonate (NaAMPS) monomer and bis-acrylamide as the crosslinker. After a 15-min UV irradiation, crosslinked poly(2-acrylamido-2-methylpropanesulfonate) (PNaAMPS) was formed *in situ* through ZIP to afford the membrane PNaAMPS-PDA-ZnO@MCE.

In a third example, the ZIP strategy was used to fabricate freestanding ZnO/hydrogel composite membranes (Scheme 1C). The pores of such membranes can be generated by incorporating a pore-forming templating agent such as crystals,[50] solvents,[51] or inert polymers[52] in the membrane precursor, followed by removing the

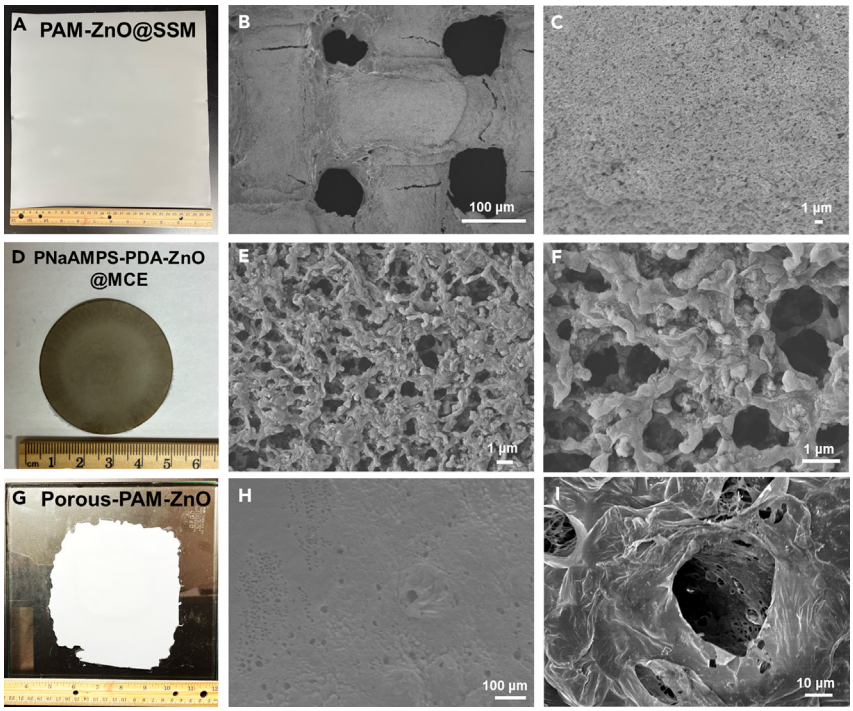

Figure 1. Photographic and SEM images of the ZIP-derived membranes

(A–C) Photographic image (A) and (B and C) SEM images of the PAM-ZnO@SSM membrane.
(D–F) Photographic image (D) and (E and F) SEM images of the PNaAMPS-PDA-ZnO@MCE membrane.
(G–I) Photographic image (G) and (H and I) SEM images of the porous-PAM-ZnO membrane.
Rulers in (A), (D), and (G) are marked in centimeters.

templating agent after the formation of the membrane.[53] Such a freestanding membrane can remove emulsified oil droplets and degrade dissolved organic pollutants from water simultaneously. On the one hand, the ZnONPs impart high local roughness and hence endow the membrane with superhydrophilicity and underwater superoleophobicity. On the other hand, the high composition of ZnONPs in the freestanding membrane provides a sufficiently tortuous path for dissolved organic molecules passing through the membrane to approach in close proximity to ZnONPs for photodegradation. To fabricate a porous membrane, we dispersed 500 nm-sized ZnONPs in a 3-wt. % solution of polyethylene glycol (PEG, MW = 20 kg/mol). PEG functions as both the surfactant to reduce ZnONPs agglomeration in water[54] and as the pore-forming agent of the membrane.[52] Acrylamide and bis-acrylamide were then dissolved into the suspension, which was subsequently cast onto a glass substrate and sandwiched between two pieces of glass spaced by 200-μm-thick microcover glass slides for the control of the membrane thickness. Following UV curing for 20 min, the as-synthesized membrane was separated from the glass plates and soaked in warm water for 48 h to afford the freestanding porous-PAM-ZnO membrane.

Morphology and surface wettability

The morphologies of all three classes of membranes were characterized by scanning electron microscopy (SEM) (Figure 1). SEM images of the PAM-ZnO@SSM membrane showed uniform coverage of the mesh wire with a highly rough layer of ZnONPs integrated with the PAM hydrogel matrix (Figures 1B, 1C, and S2). Significantly, the coating was not observed on the inner walls of the mesh pores, and thus the pore channels for water passage remain unobstructed by the coating material,

thereby ensuring a high water flux during filtration. This advantageous distribution of the coating underscores the benefits of using photopolymerization in such applications.[26]

Characterization data were collected throughout the fabrication of the PNaAMPS-PDA-ZnO@MCE membrane from its initial MCE precursor. The pristine MCE membrane displayed a white color with interconnected pores of ~0.45 μm in diameter (Figures S3A and S3B). Upon the deposition of ZnONPs and PDA, the membrane turned dark brown. SEM imaging revealed a substantial number of nanoscale ZnONPs immobilized on the MCE fibers (illustrated in Figures S3C–S3F), resulting in a noticeably rougher surface on the individual fibers. The subsequent ZIP reaction of NaAMPS caused little change in the optical membrane appearance, although SEM images (Figures 1E and 1F) revealed the formation of a hydrogel layer on the surface of ZnO-deposited fibers that reduced the average pore size while retaining the roughness. In addition, energy-dispersive X-ray spectra of the PNaAMPS-PDA-ZnO@MCE membrane provided element mapping of N, S, Na, and Zn (Figure S4), confirming the uniform distribution of ZnONPs and PNaAMPS hydrogel on the MCE fibers, leaving the pores unobstructed. Here, the excellent spatial control of the ZIP reaction was critical to keep the pores in PNaAMPS-PDA-ZnO@MCE unobstructed, even though the reaction was performed with the membrane submerged in the monomer solution.

The freestanding porous-PAM-ZnO membrane displayed a uniform white color (Figure 1G), which indicated a good dispersion of ZnONPs thanks to the presence of PEG in the fabrication process. SEM images of the porous-PAM-ZnO membrane (Figure 1H) revealed a large number of macropores with diameters of several micrometers and the presence of smaller submicrometer-sized pores (Figure 1I), which can enable a "size-sieving" effect to reject nanometer-sized emulsified oil droplets. In contrast, a control membrane without adding PEG before the ZIP reaction exhibited no macropores (Figures S5A and S5B). Another control membrane with 6 wt. % added PEG showed large pore sizes on the tens of micrometers scale (Figures S5C and S5D). Due to the mismatch in pore sizes, these control membranes failed to efficiently separate oil-in-water emulsions.

Wettability of all ZIP-fabricated membranes was evaluated by measuring water contact angles (WCAs) and underwater oil contact angles (OCAs). All three types of membranes exhibited superhydrophilicity, as evidenced by the rapid spread of water droplets within a short period of time (Figure 2A). Among them, PAM-ZnO@SSM and PNaAMPS-PDA-ZnO@MCE can be completely wetted by water droplets, with the WCA decreasing to 0° within 0.75 and 3 s, respectively. The freestanding porous-PAM-ZnO membrane exhibited a slightly higher WCA of 6.50° after 10 s. Meanwhile, all of the underwater OCAs (measured with various oils and organics solvents) of these membranes were >155° (Figures 2B, 2E, and 2F), implying outstanding underwater superoleophobicity. For example, the underwater chloroform contact angles for PAM-ZnO@SSM, PNaAMPS-PDA-ZnO@MCE, and porous-PAM-ZnO membranes were found to be 164.6° ± 2.9°, 155.0° ± 1.0°, and 157.2° ± 0.6°, respectively. The remarkable superwettability can be attributed to the synergistic effect of high surface energy hydrogel and the high surface roughness induced by ZnONPs. To validate this claim, we also synthesized control hydrogel membranes without ZnONPs using a common organic photoinitiator, Irgacure 2959 (Figure S6). These control membranes displayed significantly lower underwater chloroform contact angles of 139.8° ± 1.8°, 149.0° ± 2.4°, and 148.8° ± 1.6°, respectively (Figure S7). These results demonstrate the essential role of rough

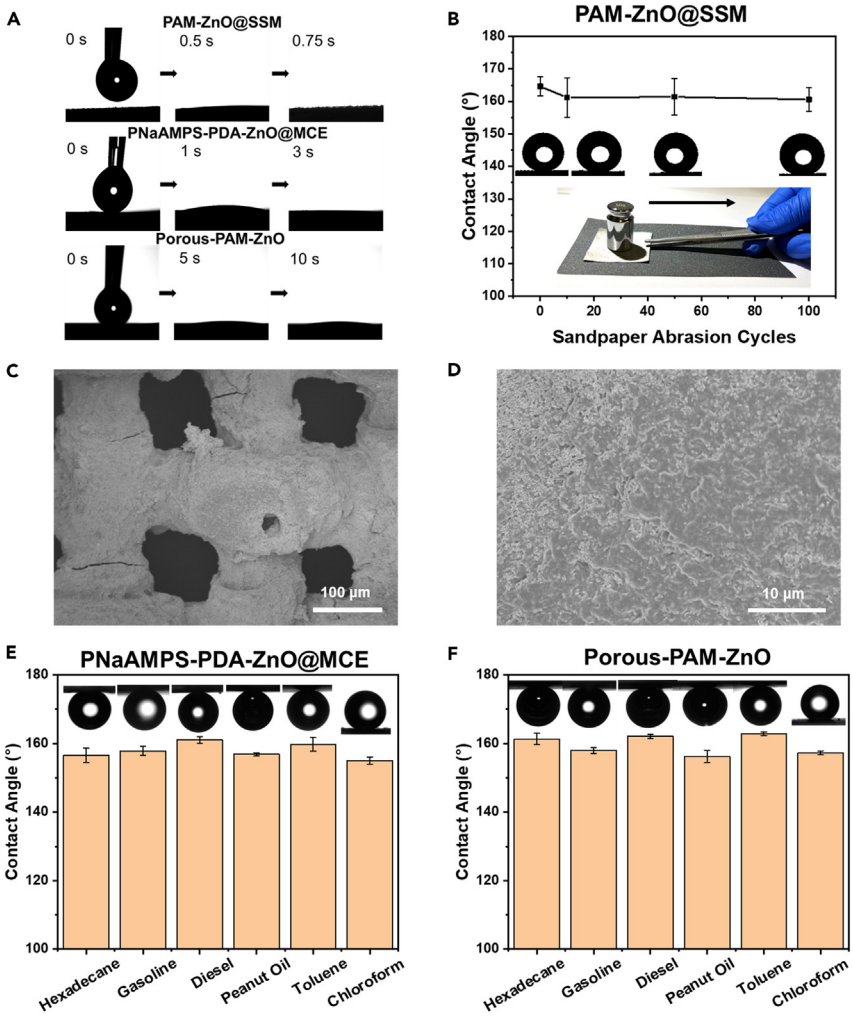

Figure 2. Surface wetting properties of ZIP-derived membranes and effect of mechanical abrasion

(A) WCAs of the ZIP-derived ZnO/hydrogel coatings.

(B) Variation of the underwater chloroform contact angles of the PAM-ZnO@SSM membrane with increasing sandpaper abrasion cycles at 6.3 kPa.

(C and D) SEM images of the PAM-ZnO@SSM membrane after 100 sandpaper abrasion cycles.

(E) Underwater OCAs of the PNaAMPS-PDA-ZnO@MCE membrane.

(F) Underwater OCAs of the porous-PAM-ZnO membrane.

The error bars in (B), (E), and (F) represent SDs calculated from triplicate experiments.

surfaces promoted by ZnONPs, which can trap water molecules and significantly reduce the oil-solid contact interface area, leading to superior underwater superoleophobicity.

The mechanical durability of membranes is critically important for their long-term use in real-world applications. Through the ZIP coating strategy presented here, a hydrogel is generated *in situ* on the surface of ZnONPs, interconnecting these nanoparticles to form an integrated ZnO/hydrogel composite layer. The hydrogel matrix provides protection and adhesion for the surface roughness, thereby enhancing the durability of the coatings. Furthermore, the rough nature of the ZnONPs layer persists even if the top layer is eroded or abraded, due to the presence of similar ZnONPs/hydrogel composite deeper in the coating. In contrast, most

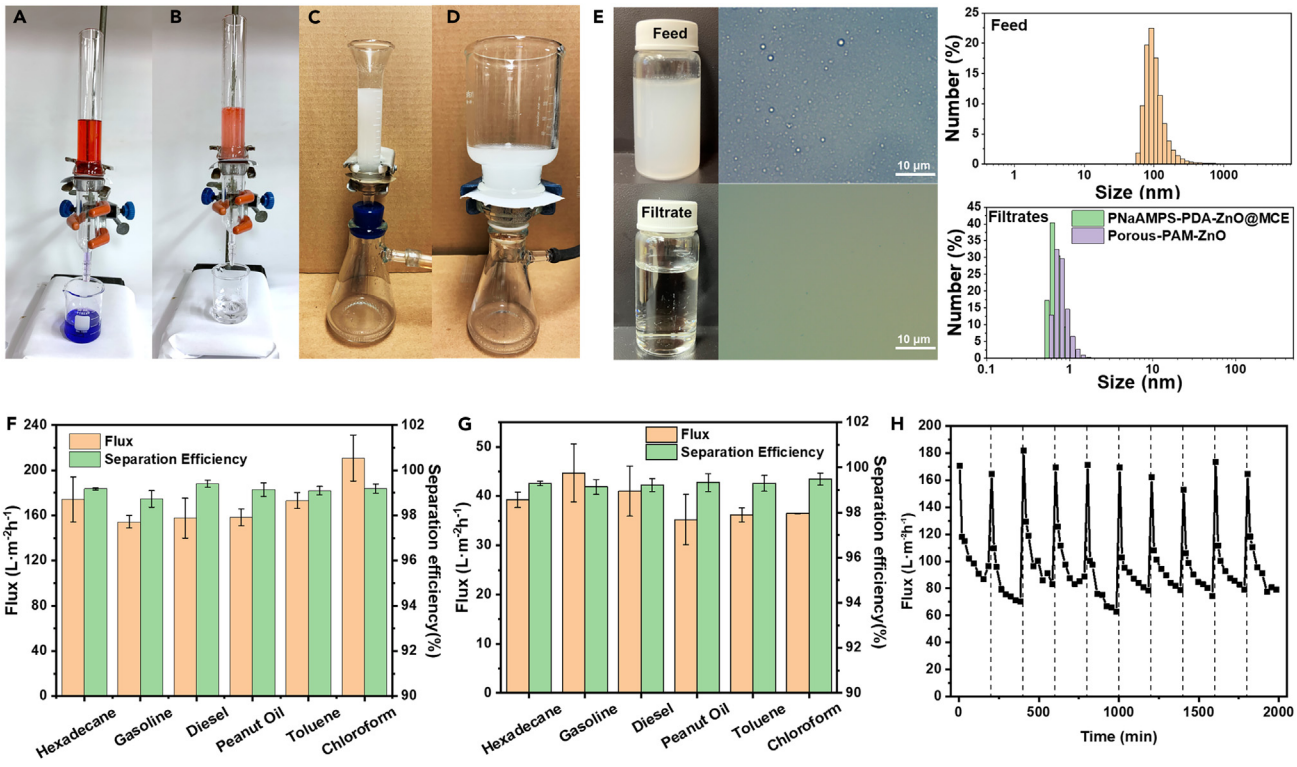

Figure 3. Separation performance of the ZIP-derived membranes in purifying stratified oil/water mixture and nanoscale oil-in-water emulsions

(A–D) Photographs of the separation process of (A) stratified hexadecane/water mixture and (B) surfactant-free hexadecane/water emulsion using the PAM-ZnO@SSM membrane, as well as the separation of surfactant-stabilized hexadecane/water emulsion using (C) PNaAMPS-PDA-ZnO@MCE membrane and (D) porous-PAM-ZnO membrane.

(E) Photographic and optical microscope images and droplet size distribution of the water sample before and after the separation shown in (C) and (D).

(F and G) Fluxes and separation efficiencies of various SDS-stabilized oil-in-water emulsions using the (F) PNaAMPS-PDA-ZnO@MCE membrane and (G) porous-PAM-ZnO membrane.

(H) Flux variation of the PNaAMPS-PDA-ZnO@MCE membrane during 10 separation cycles for SDS-stabilized hexadecane/water emulsion.

The error bars in (E) and (G) represent SDs calculated from triplicate experiments.

nanoparticle-derived, rough surface structures fabricated via methods such as spray coating or hydrothermal reactions are vulnerable to damage by external effects, leading to poor mechanical durability in practical applications.[55,56] To verify this assertion, we subjected a PAM-ZnO@SSM membrane to a sandpaper abrasion test. After being abraded on 500-grit sandpaper for 100 cycles under 6.3 kPa pressure, the PAM-ZnO@SSM membrane retained its underwater chloroform OCA of >160° (Figure 2B). Although the surface morphology of the membrane appeared visibly flattened (Figure 2C), a closer examination (Figure 2D) distinctly showed that the nanoscale roughness was preserved because the rough nature of the ZnONPs extends from the surface deeper into the coating.

Oil/water separation

The oil/water separation performance of the PAM-ZnO@SSM membrane was first investigated by testing the separation of stratified hexadecane/water mixture using a setup with the membrane fixed between two glass tubes. Upon the contact of hexadecane/water mixture with the membrane, water permeated through readily while hexadecane was retained above (Figure 3A; Video S1). Fast separation was achieved with a water flux of ~19,700 L $m^{-2}h^{-1}$ under gravity, and the oil content in the water after separation was <0.5 ppm, yielding a removal efficiency >99.9% as analyzed by a total organic carbon analyzer. The oil intrusion pressure of the membrane was

measured to be higher than 1.63 kPa (Equation S1; Figure S8), suggesting good pressure tolerance of the membrane for practical applications. Furthermore, the mesh could effectively separate a surfactant-free hexadecane/water emulsion (v/v = 1:5) with droplet sizes larger than its pore size, achieving a flux of 1,340 L $m^{-2}h^{-1}$ and an efficiency >99.9% (Video S2). During the membrane filtration process, oil droplets initially came into contact with the superoleophobic mesh and were repelled. This process led to the coalescence of these droplets into larger droplets, facilitating demulsification and ultimately leading to efficient separation of these small droplet oil emulsions from water.

Featuring much smaller pore sizes, PNaAMPS-PDA-ZnO@MCE and porous-PAM-ZnO membranes are suitable for the separation of surfactant-stabilized oil-in-water emulsions with microscale/nanoscale oil droplets. These emulsion mixtures represent a more common and challenging scenario in real-world applications. Each of these membranes was tested to separate SDS-stabilized, various oil-in-water emulsions (v/v = 1:99) comprising hexadecane, gasoline, diesel, peanut oil, toluene, or chloroform, in a filtration device at a vacuum pressure of 0.08 MPa (Figures 3C and 3D; Videos S3 and S4). The feed and their filtrates were characterized by photographic and optical microscope images and dynamic light scattering (Figure 3E). Here, the case of SDS/hexadecane/water emulsion separation is used as an example to illustrate the filtration performance. After passing through the membrane, the originally milky feed became clear, and the small oil droplets (size distribution from 70 nm to 6 μm with a peak at ~100 nm) were no longer observed in the filtrate. The exact oil rejection rates of emulsified hexadecane, gasoline, diesel, peanut oil, toluene, and chloroform by the porous-PAM-ZnO membrane were determined to be 99.29%, 99.13%, 99.22%, 99.32%, 99.30%, and 99.48%, respectively, whereas the rejection rates of these solvents by PNaAMPS-PDA-ZnO@MCE were 99.18%, 98.73%, 99.40%, 99.15%, 99.10%, and 99.19%, respectively (Figures 3F and 3G). In comparison, untreated pristine MCE membranes exhibited very low separation efficiency with a water flux of ~400 L $m^{-2}h^{-1}$. Water fluxes through the PNaAMPS-PDA-ZnO@MCE membrane ranged from 154 to 210 L $m^{-2}h^{-1}$, representing only an ~50% decrease from the pristine MCE membrane after PDA/ZnO deposition and ZIP, thanks to the spatial control of the ZIP reaction. Finally, as expected, the freestanding porous-PAM-ZnO membrane demonstrated lower water fluxes of 36–44 L $m^{-2}h^{-1}$. This low flux was anticipated because of the much smaller pore volume of this membrane, and indeed it is a representation of the greater tortuosity of the flow pathways. This is in fact desirable for the application of flow-through photodegradation of dissolved organic pollutants.

Membrane fouling by the accumulation of oil on the membrane is a critical challenge in oil/water separation, which can lead to the decline in separation performance. To investigate the antifouling property and cyclability of the ZIP-fabricated membranes, water fluxes of PNaAMPS-PDA-ZnO@MCE membrane were recorded over time during 10 cycles of the separation of SDS-stabilized hexadecane-in-water emulsion (Figure 3H). Within 3 h of each separation cycle, the water flux gradually decreased from ~170 L $m^{-2}h^{-1}$ and stabilized at ~80 L $m^{-2}h^{-1}$, resulting in an average total flux decline ratio (Equation S4) of 52.9%. The membrane was subsequently subjected to straightforward hydraulic washing to rejuvenate its surface. As a result, the permeating flux exhibited an almost complete recovery, with an average flux recovery ratio of 99.8% (Equation S5) across 10 cycles. The impressive durability and superwettability of the ZnONPs/hydrogel coating are believed to be instrumental in maintaining this membrane performance. Consequently, this membrane, enhanced with superior antifouling capabilities and reusability thanks to the superhydrophilic and

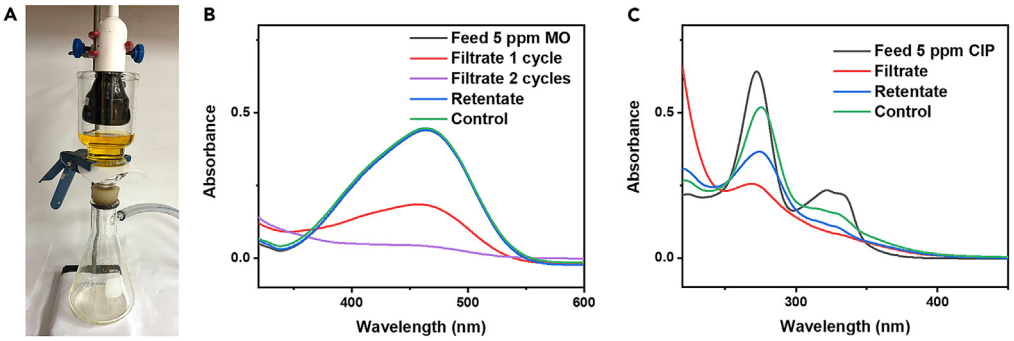

Figure 4. Flow-through photodegradation of organic contaminants by porous-PAM-ZnO membrane

(A) The filtration setup under UV irradiation of 100 mW/cm^2 at 365 nm.

(B and C) UV-vis spectra of the feed, filtrate, and control solutions, with (B) 5 ppm MO and (C) 5 ppm CIP as feed solutions.

underwater superoleophobic coating, positions itself as a promising material for practical oil-in-water emulsion separation.

Flow-through photodegradation of organic pollutants

The presence of photocatalytically active ZnONPs in porous-PAM-ZnO and the relatively low water flux through this membrane make it possible to photodegrade dissolved organic compounds when passing through the membrane. The photodegradation activity of solute flowing through porous-PAM-ZnO membrane was evaluated on two model molecules, methyl orange (MO) and ciprofloxacin (CIP), as representative examples of dyes and antibiotic contaminants present in wastewater effluents. Figure 4A demonstrates the experimental setup under UV light. It is noteworthy that the porous-PAM-ZnO membrane can readily adsorb organic compounds from the aqueous solution as a result of its porous nature. The adsorption can interfere with the photodegradation experiment because it often results in almost complete removal of both MO and CIP in the first 10 mL feed solution even without UV irradiation (Figure S9). To rule out the effect of adsorption and assess the true flow-through photodegradation efficiency under continuous operation, the membrane was immersed in 5 ppm stock solutions of MO or CIP in darkness overnight to saturate it before testing. During the test, the feed solutions were allowed to permeate through the membrane under 0.08 MPa vacuum pressure with the irradiation of 50 mW/cm^2 UV light at 365 nm, and the filtrate solution was collected continuously at a flux of 51 L m^{-2}h^{-1}. The UV-visible light (UV-vis) absorption spectra (Figures 4B and 4C) of the filtrate demonstrated a significant decrease in the peak intensity of MO and CIP by 60.2% and 60.7% in a single filtration cycle, respectively. These photodegradation efficiencies were much higher than those measured in the retentate (0% and 43.4%), which were also under UV irradiation during the experiment. The MO filtrate was further used as the feed solution for a second UV-irradiated filtration cycle, and resulted in an accumulated degradation efficiency of 90.2%. In addition, control experiments of UV irradiation of the aqueous solution of MO and CIP without the photocatalytic membranes showed only 0% and 19.2% of photodegradation within the same period of time, respectively. The greatly enhanced photodegradation performance of the flow-through membrane process is attributed to the extensive contact of the photocatalytic ZnONPs with the organic solute molecules during filtration.

To investigate the photodegradation mechanism of the porous-PAM-ZnO membrane as a flow-through reactor, we performed electron paramagnetic resonance (EPR) spectroscopy using 5,5-dimethyl-1-pyrroline *N*-oxide (DMPO) as a radical

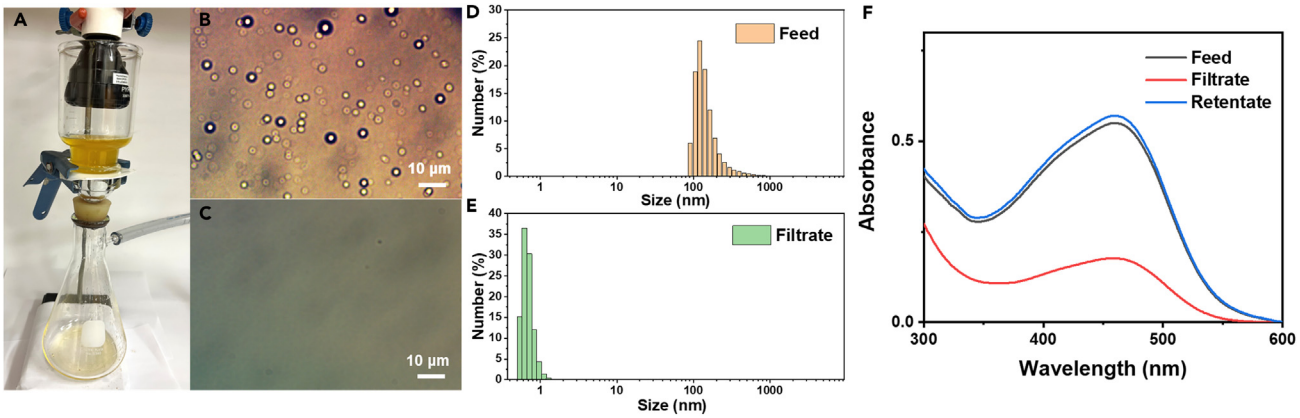

Figure 5. Simultaneous removal of dispersed and dissolved contaminants from water by the porous-PAM-ZnO membrane

(A) The setup for simultaneous removal of SDS-stabilized oil emulsion and dissolved MO from water by the porous-PAM-ZnO membrane.

(B and C) Optical images of (B) the feed SDS-stabilized hexadecane/water emulsion and (C) the filtrate.

(D and E) Droplet size distribution of (D) the feed emulsion and (E) the filtrate.

(F) UV-vis absorption spectra of the feed, filtrate, and retentate.

trapping agent. Under dark conditions, no significant EPR signal was observed from the porous-PAM-ZnO membrane sample in water. However, after UV irradiation for 5 min, a set of characteristic peaks with the intensity ratio of 1:2:2:1 was detected (Figure S10A), which is the signal of the DMPO adduct of hydroxyl radicals (•OH).[57] Therefore, the photocatalysis mechanism can be illustrated as follows (Figure S10B): on UV irradiation, excited electrons in the conduction band and oxidative holes in the valence band can react with O_2 and H_2O molecules in the solution, respectively, to generate highly reactive •OH species, which can further degrade the organic molecules absorbed in close proximity to ZnONPs through oxidation processes.

Complex wastewater treatment

The functions of oil-in-water emulsion separation and photocatalytic degradation of organic pollutants are integrated in the porous-PAM-ZnO membrane. It thereby has the potential to purify complex wastewater by removing both immiscible oils and soluble organic pollutants simultaneously. To test this, 5 ppm MO added SDS-stabilized hexadecane-in-water emulsion (v/v = 1:99) was fed through the porous-PAM-ZnO membrane with vacuum pressure and a UV lamp applied from above (Figure 5A). The filtrate was continuously collected with a flux of 38 L $m^{-2}h^{-1}$. The digital image revealed that the yellow and cloudy feed turned clear with a much lighter color after filtration. This process effectively removed the oil droplets (sizes ranging from 90 nm to 9 μm, average at ~150 nm) as confirmed by both optical microscopy images (Figures 5B and 5C) and dynamic light scattering data. Meanwhile, the characteristic UV-vis absorption peak of MO at 464 nm of the filtrate was reduced by 67.9% in intensity compared to the initial feed, indicating the removal of the dye after only 1 cycle of irradiation. If a cleaner removal of the dissolved organic pollutant is desired, then the filtrate can simply be recycled as the feed to go through the photodegradation again to achieve a lower concentration of the dissolved organic content. The ZIP-fabricated porous-PAM-ZnO membrane showcases superior performance in concurrently removing ultrasmall, emulsified oil droplets and degrading dissolved organic contaminants from water. The efficiency and performance stand on par with leading examples documented in the contemporary literature.[39–42] Moreover, the photopolymerization-based ZIP fabrication method is energy

efficient, cost-effective, and simpler, ensuring its feasibility and sustainability for scalable preparation and applications.

Conclusions

This study introduces a ZIP method for membrane fabrication, effectively using the multifaceted functionalities of ZnONPs. These functions include the ability of ZnONPs to induce significant surface roughness for superwettability and their inherent photoactivity that is integral for photochemical membrane fabrication and the photodegradation of organic pollutants. The ZIP method leverages the overarching benefits of photopolymerization techniques, including spatial control, scalability, low energy consumption, sustainability, and adaptability to a variety of substrates and fabrication scenarios. To underscore the versatility of the ZIP method, we present the fabrication of three distinct membrane types within this work. Each of these membranes demonstrates superhydrophilicity, underwater-superoleophobicity, and remarkable mechanical durability. Their efficacy is displayed through various oil/water separation applications, encompassing the separation of both stratified and emulsified oil/water mixtures. These membranes consistently show superior performance metrics: (1) high water permeance thanks to the spatial control afforded by the ZIP method, (2) exceptional oil removal efficiency due to the carefully managed pore size and underwater superoleophobicity, and (3) impressive cyclability owing to their robust mechanical resilience. Moreover, the freestanding membrane showcases a combined ability to efficiently remove emulsified oil droplets and photodegrade dissolved organic dye from water. Overall, this research illuminates a cost-effective, scalable, and sustainable membrane fabrication method with potential applicability across diverse water treatment scenarios. This versatile strategy can be expanded to encompass a broader range of semiconductor nanoparticles, monomers, and substrates. Meanwhile, it holds the potential to be integrated with advanced light-mediated membrane fabrication approaches such as large-scale photolithography and additive manufacturing. It signifies a major stride toward a sustainable future and the universal objective of achieving clean water access.

EXPERIMENTAL PROCEDURES

Resource availability

Lead contact

Further information and requests for resources and materials should be directed to and will be fulfilled by the lead contact, Lei Fang (fang@chem.tamu.edu).

Materials availability

This study did not generate new or unique reagents.

Data and code availability

All of the experimental data in this paper are available upon reasonable request from the lead contact.

Fabrication of PAM-ZnO@SSM membrane

A suspension of ZnONPs with particle sizes of ~500 nm was prepared in isopropyl alcohol (IPA) at a concentration of 20 mg/mL using probe sonication for 15 min. A horizontally placed SSM was spray-coated with the ZnO/IPA suspension using an airbrush with a 0.5-mm nozzle diameter at 1 bar pressure, until a coating density of 7 mg/cm^2 was achieved. The ZnO-coated mesh was then immersed in an aqueous solution of AM (0.4 g/mL) and bis-acrylamide (BAM, 6 mg/mL) for 10 min. After carefully removing the mesh from the monomer solution and absorbing the excess

solution from the edges with a paper towel, UV irradiation of 100 mW/cm^2 at 365 nm was applied to the mesh for 15 min. The resulting PAM-ZnO@SSM membrane was thoroughly rinsed with water to remove any unreacted monomers.

Fabrication of PNaAMPS-PDA-ZnO@MCE membrane

A total of 100 mg ZnONPs with particle sizes ~100 nm were dispersed in 50 mL Tris buffer solution (pH 8.50) using 30 W probe sonication for 30 min. Subsequently, 100 mg DA was added to the ZnO aqueous suspension and sonicated for 5 min. MCE membranes were prewetted with water and then immersed in the above suspension and stirred at 200 rpm for 24 h to achieve the PDA-ZnO@MCE membrane. Then, 5 g AMPS and 50 mg BAM were dissolved in 10 mL water and neutralized with NaOH to obtain the NaAMPS solution. The PDA-ZnO@MCE membrane was dipped in this solution for 10 min, and UV irradiation of 100 mW/cm^2 was applied to the immersed membrane for 15 min. The fabricated PNaAMPS-PDA-ZnO@MCE was washed thoroughly with methanol and water.

Fabrication of porous-PAM-ZnO membrane

A total of 200 mg ZnONPs with particle sizes ~500 nm and 300 mg PEG 20000 were added into 8 mL water and dispersed by 30 W probe sonication for 15 min. A solution containing 1 g of AM and 15 mg of BAM dissolved in 2 mL of water was then added to the dispersed ZnONPs suspension. The resulting mixture was drop cast onto a clean glass plate, and two microcover glasses with a thickness of 0.12–0.17 mm were placed on either side as spacers, which were then sandwiched by another glass plate. Subsequently, they were exposed to UV irradiation of 100 mW/cm^2 at 365 nm for 20 min and a freestanding PAM-ZnO membrane was separated from the glass plates by water flushing. Finally, the porous-PAM-ZnO membrane was obtained after soaking in warm water for 48 h to remove PEG, and the water was exchanged several times a day to facilitate elution.

SUPPLEMENTAL INFORMATION

Supplemental information can be found online at https://doi.org/10.1016/j.matt.2023.12.033.

ACKNOWLEDGMENTS

The authors acknowledge the President's X-Grants Initiative at Texas A&M University, the Robert A. Welch Foundation (A-1898 and A-1978), and the Qatar National Priority Research Program (NPRP10-0111-170152) for financial support of this work. S.S. and S.B. gratefully acknowledge partial support from the National Science Foundation under award no. IIP 2122604.

AUTHOR CONTRIBUTIONS

Conceptualization, C.L. and L.F.; methodology, C.L. and B.L.; investigation, C.L., B.J., B.L., G.Y., W.Z., and H.C.; resources, S.S., M.A., S.B., and L.F.; writing – original draft, C.L. and L.F.; writing – review & editing, C.L., S.S., G.Y., S.B., and L.F.; funding acquisition, M.A., S.B., and L.F.; supervision, S.B. and L.F.

DECLARATION OF INTERESTS

The authors declare no competing interests.

DECLARATION OF GENERATIVE AI AND AI-ASSISTED TECHNOLOGIES IN THE WRITING PROCESS

During the preparation of this work the authors used ChatGPT to improve the language and readability of the manuscript. After using this service, the authors reviewed and edited the content as needed and take full responsibility for the content of the publication.

Received: June 14, 2023
Revised: October 9, 2023
Accepted: December 20, 2023
Published: January 22, 2024

REFERENCES

1. Peterson, C.H., Rice, S.D., Short, J.W., Esler, D., Bodkin, J.L., Ballachey, B.E., and Irons, D.B. (2003). Long-Term Ecosystem Response to the Exxon Valdez Oil Spill. Science *302*, 2082–2086.

2. Shannon, M.A., Bohn, P.W., Elimelech, M., Georgiadis, J.G., Mariñas, B.J., and Mayes, A.M. (2008). Science and technology for water purification in the coming decades. Nature *452*, 301–310.

3. Pal, A., Gin, K.Y.-H., Lin, A.Y.-C., and Reinhard, M. (2010). Impacts of emerging organic contaminants on freshwater resources: Review of recent occurrences, sources, fate and effects. Sci. Total Environ. *408*, 6062–6069.

4. Ge, J., Shi, L.-A., Wang, Y.-C., Zhao, H.-Y., Yao, H.-B., Zhu, Y.-B., Zhang, Y., Zhu, H.-W., Wu, H.-A., and Yu, S.-H. (2017). Joule-heated graphene-wrapped sponge enables fast clean-up of viscous crude-oil spill. Nat. Nanotechnol. *12*, 434–440.

5. Deshmukh, A., Boo, C., Karanikola, V., Lin, S., Straub, A.P., Tong, T., Warsinger, D.M., and Elimelech, M. (2018). Membrane distillation at the water-energy nexus: limits, opportunities, and challenges. Energy Environ. Sci. *11*, 1177–1196.

6. An, C., Huang, G., Yao, Y., and Zhao, S. (2017). Emerging usage of electrocoagulation technology for oil removal from wastewater: A review. Sci. Total Environ. *579*, 537–556.

7. Huber, M.M., Canonica, S., Park, G.-Y., and von Gunten, U. (2003). Oxidation of Pharmaceuticals during Ozonation and Advanced Oxidation Processes. Environ. Sci. Technol. *37*, 1016–1024.

8. Lee, C.S., Robinson, J., and Chong, M.F. (2014). A review on application of flocculants in wastewater treatment. Process Saf. Environ. Protect. *92*, 489–508.

9. Pendergast, M.M., and Hoek, E.M. (2011). A review of water treatment membrane nanotechnologies. Energy Environ. Sci. *4*, 1946–1971.

10. Yin, J., and Deng, B. (2015). Polymer-matrix nanocomposite membranes for water treatment. J. Membr. Sci. *479*, 256–275.

11. Tanudjaja, H.J., Hejase, C.A., Tarabara, V.V., Fane, A.G., and Chew, J.W. (2019). Membrane-based separation for oily wastewater: A practical perspective. Water Res. *156*, 347–365.

12. Rivera-Gonzalez, N., Bajpayee, A., Nielsen, J., Zakira, U., Zaheer, W., Handy, J., Sill, T., Birgisson, B., Bhatia, M., and Banerjee, S. (2022). Textured ceramic membranes for desilting and deoiling of produced water in the Permian Basin. iScience *25*, 105063.

13. Xue, Z., Cao, Y., Liu, N., Feng, L., and Jiang, L. (2014). Special wettable materials for oil/water separation. J. Mater. Chem. A *2*, 2445–2460.

14. Wang, B., Liang, W., Guo, Z., and Liu, W. (2015). Biomimetic super-lyophobic and super-lyophilic materials applied for oil/water separation: a new strategy beyond nature. Chem. Soc. Rev. *44*, 336–361.

15. Chen, C., Weng, D., Mahmood, A., Chen, S., and Wang, J. (2019). Separation Mechanism and Construction of Surfaces with Special Wettability for Oil/Water Separation. ACS Appl. Mater. Interfaces *11*, 11006–11027.

16. O'Loughlin, T.E., Martens, S., Ren, S.R., McKay, P., and Banerjee, S. (2017). Orthogonal Wettability of Hierarchically Textured Metal Meshes as a Means of Separating Water. Adv. Eng. Mater. *19*, 1600808.

17. Bajpayee, A., Alivio, T.E.G., McKay, P., and Banerjee, S. (2019). Functionalized Tetrapodal ZnO Membranes Exhibiting Superoleophobic and Superhydrophilic Character for Water/Oil Separation Based on Differential Wettability. Energy Fuels *33*, 5024–5034.

18. Zarghami, S., Mohammadi, T., Sadrzadeh, M., and Van der Bruggen, B. (2019). Superhydrophilic and underwater superoleophobic membranes - A review of synthesis methods. Prog. Polym. Sci. *98*, 101166.

19. Young, T. (1805). III. An essay on the cohesion of fluids. Phil. Trans. Roy. Soc. Lond. *95*, 65–87.

20. Cassie, A.B.D., and Baxter, S. (1944). Wettability of porous surfaces. Trans. Faraday Soc. *40*, 546–551.

21. Cassie, A.B.D. (1948). Contact angles. Discuss. Faraday Soc. *3*, 11–16.

22. Yang, H.-C., Pi, J.-K., Liao, K.-J., Huang, H., Wu, Q.-Y., Huang, X.-J., and Xu, Z.-K. (2014). Silica-Decorated Polypropylene Microfiltration Membranes with a Mussel-Inspired Intermediate Layer for Oil-in-Water Emulsion Separation. ACS Appl. Mater. Interfaces *6*, 12566–12572.

23. Yang, X., He, Y., Zeng, G., Chen, X., Shi, H., Qing, D., Li, F., and Chen, Q. (2017). Bio-inspired method for preparation of multiwall carbon nanotubes decorated superhydrophilic poly(vinylidene fluoride) membrane for oil/water emulsion separation. Chem. Eng. J. *321*, 245–256.

24. Dong, Y., Li, J., Shi, L., Wang, X., Guo, Z., and Liu, W. (2014). Underwater superoleophobic graphene oxide coated meshes for the separation of oil and water. Chem. Commun. *50*, 5586–5589.

25. Lv, Y., Xi, X., Dai, L., Tong, S., and Chen, Z. (2021). Hydrogel as a Superwetting Surface Design Material for Oil/Water Separation: A Review. Adv. Mater. Interfac. *8*, 2002030.

26. Xue, Z., Wang, S., Lin, L., Chen, L., Liu, M., Feng, L., and Jiang, L. (2011). A Novel Superhydrophilic and Underwater Superoleophobic Hydrogel-Coated Mesh for Oil/Water Separation. Adv. Mater. *23*, 4270–4273.

27. Fan, J.-B., Song, Y., Wang, S., Meng, J., Yang, G., Guo, X., Feng, L., and Jiang, L. (2015). Directly Coating Hydrogel on Filter Paper for Effective Oil–Water Separation in Highly Acidic, Alkaline, and Salty Environment. Adv. Funct. Mater. *25*, 5368–5375.

28. Zhu, Y., Wang, J., Zhang, F., Gao, S., Wang, A., Fang, W., and Jin, J. (2018). Zwitterionic Nanohydrogel Grafted PVDF Membranes with Comprehensive Antifouling Property and Superior Cycle Stability for Oil-in-Water Emulsion Separation. Adv. Funct. Mater. *28*, 1804121.

29. Gao, S., Chen, J., Zheng, Y., Wang, A., Dong, D., Zhu, Y., Zhang, Y., Fang, W., and Jin, J. (2022). Gradient Adhesive Hydrogel Decorated Superhydrophilic Membranes for Ultra-Stable Oil/Water Separation. Adv. Funct. Mater. *32*, 2205990.

30. Wang, Z., Guo, P., Heng, L., and Jiang, L. (2021). Nano/submicrometer-emulsion oily wastewater treatment inspired by plant transpiration. Matter *4*, 1274–1286.

31. Chong, M.N., Jin, B., Chow, C.W.K., and Saint, C. (2010). Recent developments in photocatalytic water treatment technology: A review. Water Res. *44*, 2997–3027.

32. Ahmed, F.U., Upadhaya, D., Dhar Purkayastha, D., and Krishna, M.G. (2022). Stable hydrophilic

and underwater superoleophobic ZnO nanorod decorated nanofibrous membrane and its application in wastewater treatment. J. Membr. Sci. *659*, 120803.

33. Sun, A., Zhan, Y., Feng, Q., Yang, W., Dong, H., Liu, Y., Chen, X., and Chen, Y. (2022). Assembly of MXene/ZnO heterojunction onto electrospun poly(arylene ether nitrile) fibrous membrane for favorable oil/water separation with high permeability and synergetic antifouling performance. J. Membr. Sci. *663*, 120933.

34. Gao, C., Sun, Z., Li, K., Chen, Y., Cao, Y., Zhang, S., and Feng, L. (2013). Integrated oil separation and water purification by a double-layer TiO2-based mesh. Energy Environ. Sci. *6*, 1147–1151.

35. Yan, S., Li, Y., Xie, F., Wu, J., Jia, X., Yang, J., Song, H., and Zhang, Z. (2020). Environmentally Safe and Porous MS@TiO2@PPy Monoliths with Superior Visible-Light Photocatalytic Properties for Rapid Oil–Water Separation and Water Purification. ACS Sustain. Chem. Eng. *8*, 5347–5359.

36. Ma, L., He, J., Wang, J., Zhou, Y., Zhao, Y., Li, Y., Liu, X., Peng, L., and Qu, M. (2019). Functionalized Superwettable Fabric with Switchable Wettability for Efficient Oily Wastewater Purification, in Situ Chemical Reaction System Separation, and Photocatalysis Degradation. ACS Appl. Mater. Interfaces *11*, 43751–43765.

37. Zhang, L., Gu, J., Song, L., Chen, L., Huang, Y., Zhang, J., and Chen, T. (2016). Underwater superoleophobic carbon nanotubes/core–shell polystyrene@Au nanoparticles composite membrane for flow-through catalytic decomposition and oil/water separation. J. Mater. Chem. A *4*, 10810–10815.

38. Li, L., Liu, Z., Zhang, Q., Meng, C., Zhang, T., and Zhai, J. (2015). Underwater superoleophobic porous membrane based on hierarchical TiO2 nanotubes: multifunctional integration of oil–water separation, flow-through photocatalysis and self-cleaning. J. Mater. Chem. A *3*, 1279–1286.

39. Qian, D., Chen, D., Li, N., Xu, Q., Li, H., He, J., and Lu, J. (2018). TiO2/sulfonated graphene oxide/Ag nanoparticle membrane: In situ separation and photodegradation of oil/water emulsions. J. Membr. Sci. *554*, 16–25.

40. Wang, Y., Liu, Z., Wei, X., Liu, K., Wang, J., Hu, J., and Lin, J. (2021). An integrated strategy for achieving oil-in-water separation, removal, and anti-oil/dye/bacteria-fouling. Chem. Eng. J. *413*, 127493.

41. Bao, Z., Chen, D., Li, N., Xu, Q., Li, H., He, J., and Lu, J. (2020). Superamphiphilic and underwater superoleophobic membrane for oil/water emulsion separation and organic dye degradation. J. Membr. Sci. *598*, 117804.

42. You, X., Wang, M., Jiang, G., Zhao, X., Wang, Z., Liu, F., Zhao, C., Qiu, Z., and Zhao, R. (2023). Multifunctional porous nanofibrous membranes with superior antifouling properties for oil-water separation and photocatalytic degradation. J. Membr. Sci. *668*, 121245.

43. Zheng, X., Wu, D., Su, T., Bao, S., Liao, C., and Wang, Q. (2014). Magnetic Nanocomposite Hydrogel Prepared by ZnO-initiated Photopolymerization for La (III) Adsorption. ACS Appl. Mater. Interfaces *6*, 19840–19849.

44. Li, C., Lee, B., Wang, C., Bajpayee, A., Douglas, L.D., Phillips, B.K., Yu, G., Rivera-Gonzalez, N., Peng, B.-j., Jiang, Z., et al. (2022). Photopolymerized superhydrophobic hybrid coating enabled by dual-purpose tetrapodal ZnO for liquid/liquid separation. Mater. Horiz. *9*, 452–461.

45. Schmitt, M. (2015). Synthesis and testing of ZnO nanoparticles for photo-initiation: experimental observation of two different non-migration initiators for bulk polymerization. Nanoscale *7*, 9532–9544.

46. Shaban, M., Poostforooshan, J., and Weber, A.P. (2017). Surface-initiated polymerization on unmodified inorganic semiconductor nanoparticles via surfactant-free aerosol-based synthesis toward core–shell nanohybrids with a tunable shell thickness. J. Mater. Chem. A *5*, 18651–18663.

47. Zhang, Q., Liu, N., Wei, Y., and Feng, L. (2018). Facile fabrication of hydrogel coated membrane for controllable and selective oil-in-water emulsion separation. Soft Matter *14*, 2649–2654.

48. Li, D., Huang, X., Huang, Y., Yuan, J., Huang, D., Cheng, G.J., Zhang, L., and Chang, C. (2019). Additive Printed All-Cellulose Membranes with Hierarchical Structure for Highly Efficient Separation of Oil/Water Nanoemulsions. ACS Appl. Mater. Interfaces *11*, 44375–44382.

49. Cao, J., Su, Y., Liu, Y., Guan, J., He, M., Zhang, R., and Jiang, Z. (2018). Self-assembled MOF membranes with underwater superoleophobicity for oil/water separation. J. Membr. Sci. *566*, 268–277.

50. Dadsetan, M., Hefferan, T.E., Szatkowski, J.P., Mishra, P.K., Macura, S.I., Lu, L., and Yaszemski, M.J. (2008). Effect of hydrogel porosity on marrow stromal cell phenotypic expression. Biomaterials *29*, 2193–2202.

51. Butler, R., Hopkinson, I., and Cooper, A.I. (2003). Synthesis of Porous Emulsion-Templated Polymers Using High Internal Phase CO2-in-Water Emulsions. J. Am. Chem. Soc. *125*, 14473–14481.

52. Zhao, K., Zhang, X., Wei, J., Li, J., Zhou, X., Liu, D., Liu, Z., and Li, J. (2015). Calcium alginate hydrogel filtration membrane with excellent anti-fouling property and controlled separation performance. J. Membr. Sci. *492*, 536–546.

53. Yang, Q., Adrus, N., Tomicki, F., and Ulbricht, M. (2011). Composites of functional polymeric hydrogels and porous membranes. J. Mater. Chem. *21*, 2783–2811.

54. El-Shazly, A.N., Rashad, M.M., Abdel-Aal, E.A., Ibrahim, I.A., El-Shahat, M.F., and Shalan, A.E. (2016). Nanostructured ZnO photocatalysts prepared via surfactant assisted Co-Precipitation method achieving enhanced photocatalytic activity for the degradation of methylene blue dyes. J. Environ. Chem. Eng. *4*, 3177–3184.

55. Zheng, W., Huang, J., Li, S., Ge, M., Teng, L., Chen, Z., and Lai, Y. (2021). Advanced Materials with Special Wettability toward Intelligent Oily Wastewater Remediation. ACS Appl. Mater. Interfaces *13*, 67–87.

56. Zhang, W., Wang, D., Sun, Z., Song, J., and Deng, X. (2021). Robust superhydrophobicity: mechanisms and strategies. Chem. Soc. Rev. *50*, 4031–4061.

57. Brezová, V., Gabcová, S., Dvoranová, D., and Staško, A. (2005). Reactive oxygen species produced upon photoexcitation of sunscreens containing titanium dioxide (an EPR study). J. Photochem. Photobiol., B *79*, 121–134.